



Evaluation of Toxicological Effects of ZnO and CuO Nanoparticles with *Taraxacum officinale* as Bioindicator

Paulina Abrica-González · Sandra Gómez-Arroyo ·
Arón Jazcilevich-Diamant · Antonio Sotelo-López ·
Ana Rosa Flores-Márquez · Josefina Cortés-Eslava

Received: 9 January 2023 / Accepted: 9 June 2023 / Published online: 1 July 2023
© The Author(s) 2023

Abstract Nanoparticles are rising worries because of recent reports about potential toxicity amid the incorporation of these emerging materials into consumer products, and industrial and scientific applications. New developments in the automotive industry are incorporating novel materials, which have increased the emission of nanoparticles into the atmosphere. To overcome the difficulty of detecting and characterizing atmospheric nanoparticles, alternative methods have been proposed, just as the

indirect detection and characterization with bioindicators. We report the use of *Taraxacum officinale* as a sentinel organism to describe the effects of atmospheric nanostructured pollutants. ZnO and CuO nanoparticles (ZnO-NPs, CuO-NPs) were selected for this study, as they are two of the most present nanomaterials in the emerging automotive industry. The physiological effect on *Taraxacum officinale* exposure to ZnO-NPs and CuO-NPs was evaluated through growth rate, and total chlorophyll content; and comet assay was performed to evaluate the DNA damage. The exposure of plants was made by nebulizing dispersions of the nanoparticles. The exposure to ZnO-NPs presented the maximum DNA damage at a concentration of 100 mg/L. The DNA damage by both studied nanoparticles showed a significant difference against its bulk counterparts. Scanning electron microscopy (SEM) micrographs showed an accumulation of nanoparticles near the stomata. The study demonstrated the feasibility of *T. officinale* as a bioindicator of air-related nanoparticles toxicity, and the high sensitivity of the comet assay for this approach.

Short synopsis: This study reports the advantages in the use of bioindicators, and comet assay, to study the effects of atmospheric nanoparticles.

P. Abrica-González (✉) · S. Gómez-Arroyo ·
A. R. Flores-Márquez · J. Cortés-Eslava
Laboratorio de Genotoxicología Ambiental, Instituto de
Ciencias de la Atmósfera y Cambio Climático, Universidad
Nacional Autónoma de México, Ciudad Universitaria,
Coyoacán 04510, Ciudad de México, México
e-mail: pabricag@ipn.mx

A. Jazcilevich-Diamant
Departamento de Ciencias Ambientales, Instituto de
Ciencias de la Atmósfera y Cambio Climático, Universidad
Nacional Autónoma de México, Ciudad Universitaria,
Coyoacán 04510, Ciudad de Mexico, México

A. Sotelo-López
Laboratorio de Técnicas Fototérmicas, Departamento
de Ciencias Básicas, Unidad Profesional
Interdisciplinaria de Biotecnología, Instituto Politécnico
Nacional, Av. Acueducto, La Laguna Ticomán,
Gustavo A. Madero 07340, Ciudad de México, México

Keywords Bioindicators · Comet assay · DNA damage · Pollution · Toxicity

1 Introduction

Air pollution in megacities is strongly influenced by topography, meteorology variables, and a wide range

of natural and anthropogenic sources, with the automotive sector accounting for the largest share of emissions (Dong et al., 2021). Particularly in the automotive industry, there is a demand and need to produce low-cost, efficient, and sustainable materials (Ibrahim et al., 2016), with nanotechnology being one of the most promising resources since it can improve different thermal, optical, magnetic, and electrical properties of the material (Abrica-González et al., 2018). Metal oxides such as MnO, ZnO, CuO, and TiO₂ are used as additives (Yuvarajan et al., 2018), and it has been reported that nanoparticles of CuO, ZnO, TiO₂, and MgO, Al₂O₃ improve thermal conductivity (Shafique & Luo, 2019). Moreover, with the rise of electric vehicles and renewable energy sources, the use of CuO and ZnO nanoparticles has increased for the development of specialized lubricants and supercapacitors for solar cells and energy storage (Khan et al., 2019; Kumar et al., 2020; Rahman & Myo Aung, 2021; Shah et al., 2022).

The emission of nanoparticles by the automotive sector has resulted in damage to living beings and ecosystems (Coelho et al., 2012), with negative effects such as tissue inflammation, cytotoxicity, oxidative stress, DNA damage, neurological problems, and other diseases (Shafique & Luo, 2019). The quantification of nanomaterials dispersed in the environment is complex, and on the other hand, the evaluation of their effects on life beings and ecosystems is a problem scarcely addressed. Previous studies have shown that remote sensing can be used to assess the environmental impact of mining facilities by analyzing green cover loss, by comparing the normalized difference vegetation index (NDVI) and normalized difference red edge index (NDRe) values from different periods (Cetin et al., 2022a). However, these studies have been limited in their ability to identify the specific types of pollutants that are causing the damage. One way to overcome this limitation is to use plants as bioindicators to detect a wide range of environmental pollutants. The utilization of bioindicators represents one of the most effective approaches for assessing the impacts of pollutants on biodiversity and the species inhabiting ecosystems (Parmar et al., 2016). This is particularly relevant in urban environments where the presence of heavy metals, such as Al, Cd, Cr, Cu, Fe, Mn, Ni, Pb, Zn, and Co, has been identified through the utilization of plants as bioindicators (Cortés-Eslava et al., 2023; Gómez-Arroyo

et al., 2018a, b; Martínez-Pérez et al., 2021). These findings have been further supported by soil analysis (Bozdogan Sert et al., 2019; Cetin et al., 2022b, c). Additionally, plants have proven to be valuable tools in estimating indoor air quality, even in indoor environments where air quality can pose risks to human health and quality of life due to the presence of particulate matter (PM) or elevated concentrations of CO₂ (Cetin, 2016a). Studies have shown that plants can indirectly estimate the concentration of indoor particulate matter, further highlighting their potential as bioindicators (Van Dyck et al., 2019). Given the complexity of the behavior of nanoparticles in the environment, plants are a good option for the study of their toxicity, as the exposition may occur by direct foliar absorption, as reported by Zhao et al. (2017) in a study where submerged leaves contributed to most of the NPs internalization, or through the roots, followed by translocation across different tissues (Lv et al., 2019; Tripathi et al., 2017). Regardless of the exposure mechanism, when nanoparticles end up inside plants or cells, they produce different toxic effects that cause abnormal behavior (Cox et al., 2016). They can cause mitochondrial damage, as has been observed with carbon nanotubes, or impair permeability as with metallic NPs (Karlsson, 2010); most of the effects caused by NPs in cells refer to oxidative stress (Martínez et al., 2020). Another factor that may contribute to the uptake of metallic nanoparticles by plants is the presence of unsaturated porous media, where interactions at the air–water–soil interfaces play important roles (Morales et al., 2011). Mostly with the presence of humic and fluvic acids that contribute to the retention of colloidal nanoparticles through the formation of stable complexes, confirming the importance of the study of airborne nanoparticles with plants as bioindicators (Adamczyk-Szabela et al., 2021).

While some metal oxides have been utilized in the development of fertilizers and have shown potential for improving growth and nitrogen fixation capacity, it is relevant to consider that they can also lead to bioaccumulation in seeds and leaves (Siddiqi & Husen, 2017). Adverse effects on germination have been reported (Lee et al., 2010), and the internalization of nanoparticles through stomata has been observed (Lv et al., 2019). Given these concerns, we investigated the potential genotoxic effects of ZnO and CuO nanoparticles in plants following exposure

to leaves through nebulization. This approach mimics a naturally occurring process in which plant leaves are exposed to airborne contaminant nanoparticles transported through atmospheric humidity and mist. Recent investigations in situ have shown that in rainy seasons, the humidity in the environment can contribute to the internalization of particulate matter through the stomata (Gómez-Arroyo et al., 2018b). For this reason, our investigation focuses on the exposure of plants to nanoparticles in nebulized aqueous dispersion at different concentrations in contrast to the same components in their non-nanometric form.

Much of the research on ZnO-NPs and CuO-NPs effects reports oxidative stress (Mukherjee et al., 2014; Wei & Wang, 2013), damage to vacuoles (Pokhrel & Dubey, 2013), and reduced root length (Ma et al., 2010a, b). Despite knowing these effects, the mechanism is still not clear, although, depending on the dimensions of the NPs, the dynamics of particle distribution through different plant structures have barely begun to be characterized (Wang et al., 2013, 2016), that is why we found important to study the effects of plants leaves exposure to airborne nanoparticles. Among other factors, concentration plays an important role; studies on soil have reported that at low concentrations (around 50 mg/kg), ZnO-NPs have favorable effects on plants. On the contrary, concentrations higher than 500 mg/kg can be harmful. Moreover, the aggregation and agglomeration of nanomaterials make it difficult to analyze the presence of nanomaterials in the environment, and although there are indications that most end up in aquatic environments (Lin et al., 2010), mainly as a result of a bad design of urban landscapes where particles are dragged by runoff storm water (Cetin, 2013), their presence in the atmosphere has raised concern. Currently, there are no studies that directly report the concentration of ZnO or CuO nanoparticles in the atmosphere. Several researchers report the presence of metals indirectly (Dzierżanowski et al., 2011; Gómez-Arroyo et al., 2018a, b; Lv et al., 2019). Usually, the reports provide the weighted mass concentration of Zn or Cu, that may not be enough for the assessment of the effect of metal oxide nanoparticles in the environment, as the diameter of this kind of nanoparticles may play a remarkable role due to the higher number concentration and surface area (Bystrzejewska-Piotrowska et al., 2009). Since there is little instrumentation for this type of determination

and given the complexity of capturing and characterizing particles smaller than 100 nm from the atmosphere, the use of plant leaves has been proposed as a tool for nanoparticle determination. Some researchers have already verified the feasibility of this method, reporting better results with small leaves and complex topology, as well as those with trichomes, epicuticular wax, or superficial ridges (Lv et al., 2019). Other studies have shown that the proper selection of certain plant species as bioindicators depends on the type of contaminant to be monitored and the growing environment (Cetin & Asghar Jawed, 2021), being able to detect the presence in the atmosphere of heavy metals such as Ba, which has been previously denied (Cetin & Asghar Jawed, 2022). One of the advantages of using plant leaves as bioindicators is that in almost every type of landscape there can be found plants that are tolerant to harsh conditions and pollutants. For the case of urban areas, the developing of landscapes with green spaces provides the enhancement of quality of life, and can be useful for the monitoring of the quality of the environment with the help of Geographic Information Systems (GIS), even improving the tourism potential of ancient cities, forest areas, and coastal areas (Cetin, 2015a, b, 2016b). After selecting suitable plants species as bioindicators and a viable methodology, environmental conditions may be evaluated as a complimentary methodology from the traditional monitoring stations.

This paper proposes the use of *Taraxacum officinale* as a bioindicator of the toxicity of metal oxide nanoparticles, by exposing plants to nebulized dispersions of ZnO and CuO nanoparticles in a closed chamber. This plant species can act as a good bioindicator due to its high tolerance to harsh environmental conditions and that it can be found widespread, also it presents a relatively high tolerance to toxic substances and low sensitivity to cumulated substances (Degórska, 2013). As a first approach, the phytotoxicity can be determined successfully by the measurement of total chlorophyll content and growth rate, but changes in these parameters may be due to different responses of the internal regulators of plants (Khataee et al., 2017), that it is important to incorporate methods more focused on DNA damage, finding in comet assay one of the best options, considering the high sensitivity of the method to detect DNA strand breaks or oxidative DNA lesions (Karlsson, 2010). Comet assay has been suggested as a good screening test for

the safety evaluation of nanomaterials, when used with biomarkers of oxidative damage to DNA (Karlsson, 2010), particularly with plant models like *Taraxacum officinale*. Comet assay test is a low-cost well-established protocol that has been used since 1990, capable of evaluating single or double strand DNA breaks at single cell level, including cross-linked protein-DNA with high reproducibility. Recently, the use of comet assay has significantly increased in the study of genotoxicity and mutagenicity induced in plants, for ecotoxicological approaches, as in the detection of environmental agents, and in the characterization of carcinogenic metals (Cortés-Eslava et al., 2018). The use of comet assay is increasing to evaluate the toxicity of nanomaterials, as these emerging contaminants have been related to DNA strand breaks and bioaccumulation. In particular, the alkaline comet assay has demonstrated great utility in assessing the effects of nanoparticles and metal oxides (Santos et al., 2015).

2 Methods

Normal melting point agarose (NMPA), EDTA (Ethylenediamine-tetraacetic acid, disodium salt $2H_2O$), and tris(hydroxymethyl)aminomethane (Tris) were purchased from Invitrogen ultraPURE. Low melting point agarose (LMPA), copper oxide nanopowder (<50 nm, Prod. No. 544868), zinc oxide nanopowder (<50, Prod. No. 677450), copper oxide powder (<10 μm , 98%), zinc oxide powder (<5 μm particle size), ethidium bromide, potassium dichromate, and sodium hydroxide, were purchased from Sigma-Aldrich. All glassware was washed with aqua regia (HCl: HNO_3 3:1 v/v) to remove any trace of metals. *Taraxacum officinale* plants were collected and adapted to laboratory conditions for one month, with 12 h light/12 h dark at 25 °C. Plants with rosette diameters of 10 and 15 cm were selected for exposure to nebulized solutions of ZnO, ZnONPs, CuO, and ZnONPs in the designed exposure chamber.

Bulk ZnO and CuO, as well as ZnO-NPs and CuO-NPs, were dispersed in distilled water at concentrations of 50, 100, 200, and 800 mg/L as treatments for plant exposure. Distilled water and potassium dichromate solution (0.05 M) were used as the negative and positive control, respectively. All solutions were sonicated for 2 h before each experiment.

2.1 Nanoparticle Characterization

The optical properties of the nanoparticles used for exposure were obtained by UV–vis absorption spectroscopy (Cintra 1010, GBC Scientific Equipment) with standard 10 mm quartz cells. Zeta potential, hydrodynamic diameter, and polydispersity index (PDI), of both ZnO-NPs and CuO-NPs, were obtained by Dynamic Light Scattering (DLS) with a Malvern Zetasizer Nanoseries (Malvern, UK) at room temperature, using DTS1060 capillary cells (Malvern Panalytical Ltd). The morphology of ZnO-NPs and CuO-NPs was characterized by scanning electron microscopy (SEM) (JSM-6390LV, JEOL, Japan). Nanopowders were mounted on SEM stubs with double-sided carbon tape, and micrographs were obtained with an accelerating voltage of 20 kV and working distance of 8.5 mm.

2.2 Plant Exposure

Cost-effective nebulization chambers were designed to expose plants to each treatment by nebulization. The chambers were custom built as 600×300×400 mm boxes of 4 mm thick poly (methyl methacrylate) (PMMA) sheets, allowing the exposure of two plants per box (Fig. 1a). The nebulizers were adapted at the top of the boxes, aligned with the long axis, 150 mm from each side. 115 kHz ultrasonic piezoelectric ceramic nebulizers (Shenzhen Electronics) were adapted to the cap of 100 mL glass vials (Fig. 1b), and the outlets of nebulizers were placed in a way that each plant gets a symmetrical and homogeneous exposure from the same distance and flow direction.

The dispersions of CuO-NPs and ZnO-NPs in distilled water were nebulized inside the chamber for plant exposure, as well as solutions of bulk CuO and ZnO at the same concentrations as references, negative control, and positive control. The outflux of each nebulizer was characterized, obtaining a flow of 0.04 L/H of 5 μm droplets, forming a nebulizing spray cone of 20° (Fig. 1c). Each exposure was performed with 50 mL of treatment dispersion per vial, for a total of 100 mL nebulized inside the chamber whose total volume is 72 L. Each treatment lasted 1.25 h, after completely emptying both vials. A different pair of plants were used for each type of treatment and for each repetition, for a total of three repetitions. After

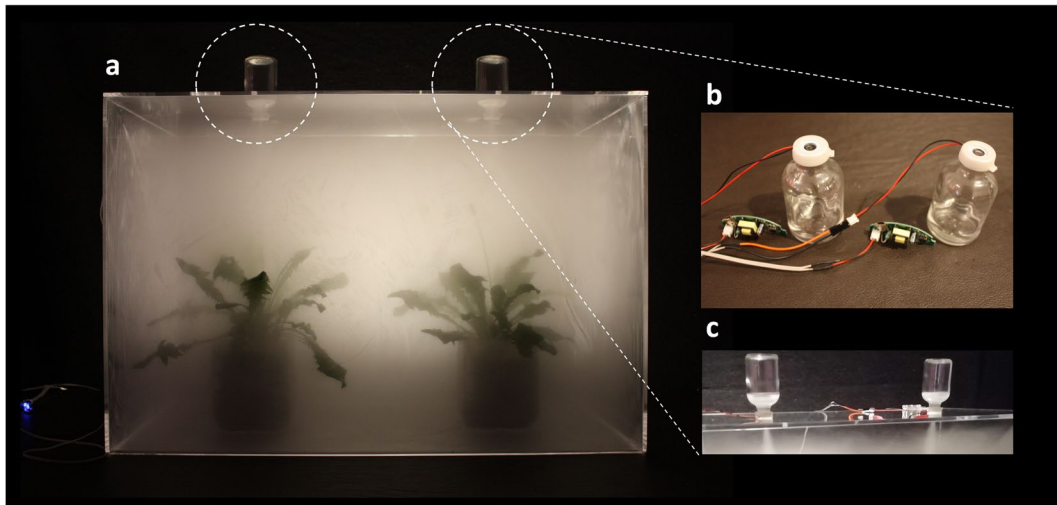


Fig. 1 Nebulization chambers built with PMMA sheets. **a** Two nebulizers were adapted at the top of the PMMA box. **b** Piezoelectric ceramic nebulizers at the cap of vials. **c** Nebulizers setup

each exposure run, the chamber was left closed until precipitation of the mist (approximately 2 h). Chambers were washed thoroughly at the end of each run.

Atmospheric data inside the chamber were registered with a datalogger (CR1000, Campbell Scientific), with humidity, temperature, and pressure transducers. Separate chambers were used for each type of treatment.

2.3 Bioaccumulation

After plant exposure, the accumulation of nanoparticles over plant leaves, and the internalization through stomata were investigated by low vacuum scanning electron microscopy (LV-SEM) (Quanta 250 FEG, FEI Thermo Fisher Scientific). The leaves were prepared directly after exposure without treatment to avoid samples contamination or loss of material from the surface. Fresh cuts of leaves of 0.5 mm × 0.5 mm were mounted in SEM stubs with double-sided carbon tape, obtaining micrographs at a pressure of 0.4 to 0.5 mbar, accelerating voltage of 15 kV, and working distance of 10.5 mm. Elemental analysis was obtained with the incorporated EDS detector. The advantage of the use of low vacuum SEM is that the samples are not modified after preparation, and the vacuum does not modify the morphology of the leaves surface.

2.4 Comet Assay

Comet assay was performed to evaluate the genotoxicity of plants exposed to nebulized nanoparticles. Three slides were prepared from each repetition, to obtain more than 100 nuclei per experiment.

2.4.1 Isolation of Nuclei from Leaves

All solutions, instruments, and glassware were stored at 4 °C before use and kept on ice during the procedure. The comet assay was performed in a darkroom with dim red light. Leaf sections of 0.5 × 4 cm were placed in glass Petri dishes (of 60 mm) with 350 μL cold 0.4 M Tris buffer (pH 7.5); the Petri dishes were kept tilted so that the nuclei could be collected by precipitation in the buffer solution after making the cuts perpendicular to the primary vein with a cold razor blade. Each sample was prepared by adding 50 μL of the nuclei suspension to 50 μL of 1% low melting point agarose (LMPA) at 40 °C and mixing gently. Subsequently, 75 μL of the mixture was placed on a coverslip to immediately overlap the slide (previously covered with 0.5% normal melting point agarose) avoiding the formation of bubbles. For the agarose to solidify, the slides were placed on a cold surface for 5 min, and the coverslip was removed. Finally, cover the preparation with a protective layer of 75 μL of 0.5% LMPA at 37 °C (Gichner & Plewa, 1998).

2.4.2 DNA Unwinding and Electrophoresis

The slides with the nuclei were incubated for 15 min with freshly prepared alkaline buffer (300 mM NaOH, 1 mM EDTA, pH > 13) to allow the DNA to unwind. Subsequently, the electrophoresis was performed in darkness, with the slides in a horizontal chamber during 20 min at 25 V and 300 mA, at 4 °C. After this, the slides were rinsed three times in a neutralization buffer (Tris 0.4 M) for 5 min each and were placed in ethanol for 5 min for fixation.

To observe the nuclei, an epifluorescence microscope (Axiostar Plus Carl Zeiss) with an excitation filter of 515–560 nm and a barrier filter of 590 nm was used. Staining was done with ethidium bromide (2 µg/mL). At least 50 nuclei per slide and three slides per experiment were analyzed. The Comet Assay IV (Perceptive Instruments) software was used for image analysis and the following parameters were used for described DNA damage: tail moment, tail intensity (%), and tail length (µm).

Comet assay results were analyzed by three-way ANOVA for each pair of ZnO and CuO treatment sets, being the bulk and nano forms, the normality of data was confirmed with the Shapiro–Wilk test. The three considered factors were treatments (ZnO vs ZnO-NPs or CuO vs CuO-NPs), concentrations (negative control, 50, 100, 200, and 800 mg/L, and positive control), and time (24 h after treatment and 5 days after treatment), $p < 0.05$ was considered statistically significant.

2.5 Growth Rate and Chlorophyll

The total surface area of plant rosettes was calculated by image analysis with ImageJ software. The relative growth rate was calculated by dividing the measured area 5 days after exposition by the area after 24 h. The content of chlorophyll per weight was obtained by extraction from 5 day-exposed plant leaves with 90% acetone (Meyer); absorbance was measured at 664.5 nm and 647 nm (VE 722–2000, Velab), before drying, and weighing the leaves. Chlorophyll content was calculated according to Eq. 1:

$$\text{total chl} = 17.9 A_{647} + 8.08 A_{664.5} \quad (1)$$

Two-way ANOVA was used for the results of total chlorophyll content, taking concentration and each pair of treatment sets as factors, ZnO vs ZnO-NPs and CuO vs CuO-NPs.

3 Results and Discussion

3.1 Nanoparticle Characterization

Figure 2 shows the SEM micrographs for both studied nanoparticles CuO-NPs (Fig. 2a), and ZnO-NPs (Fig. 2b), along with the size distribution histograms (Fig. 2e and f, respectively). Mean diameters are 63.504 nm and 52.894 nm for CuO-NPs and ZnO-NPs, respectively. UV–Vis spectrum of ZnO-NPs (Fig. 2d), scanned from 300 to 800 nm, shows a characteristic peak at 362 nm that corresponds to the characteristic absorption of ZnO-NPs, blue shifted from the absorption peak of bulk ZnO at 376 nm (Miri et al., 2019). For CuO-NPs (Fig. 2c), UV–Vis spectrum shows a characteristic peak at 390 nm that confirms the presence of CuO-NPs (Navada et al., 2020; Sharaf Zeebaree et al., 2021). Table 1 summarizes the characterized properties of CuO and ZnO nanoparticles.

The more negative zeta potential of CuO-NPs suggests better stability than ZnO-NPs (Nabila & Kanabiran, 2018). It has been reported before that the toxicity of oxide metal nanoparticles increases with the stability of the dispersion (Lv et al., 2019; Rotini et al., 2017).

3.2 Plant Exposure

Each exposure was performed for 75 min, for each treatment or nanoparticle dispersion, until emptying the pair of 50 mL treatment vials at a medium flow rate of 0.04 L/h. The maximum relative humidity inside the chamber reached 98.7%, with an external temperature of 17 °C and an internal temperature of 18 °C. The obtained droplets of 5 µm with incorporated nanoparticles are of great interest because they may form part of the respirable percentage of aerosolized droplets (Dailey et al., 2003). Five days after plant exposure, black stains could be observed in some parts of the leaves exposed to CuO-NPs and white stains in those exposed to ZnO-NPs, confirming the accumulation of nanomaterial on the surface.

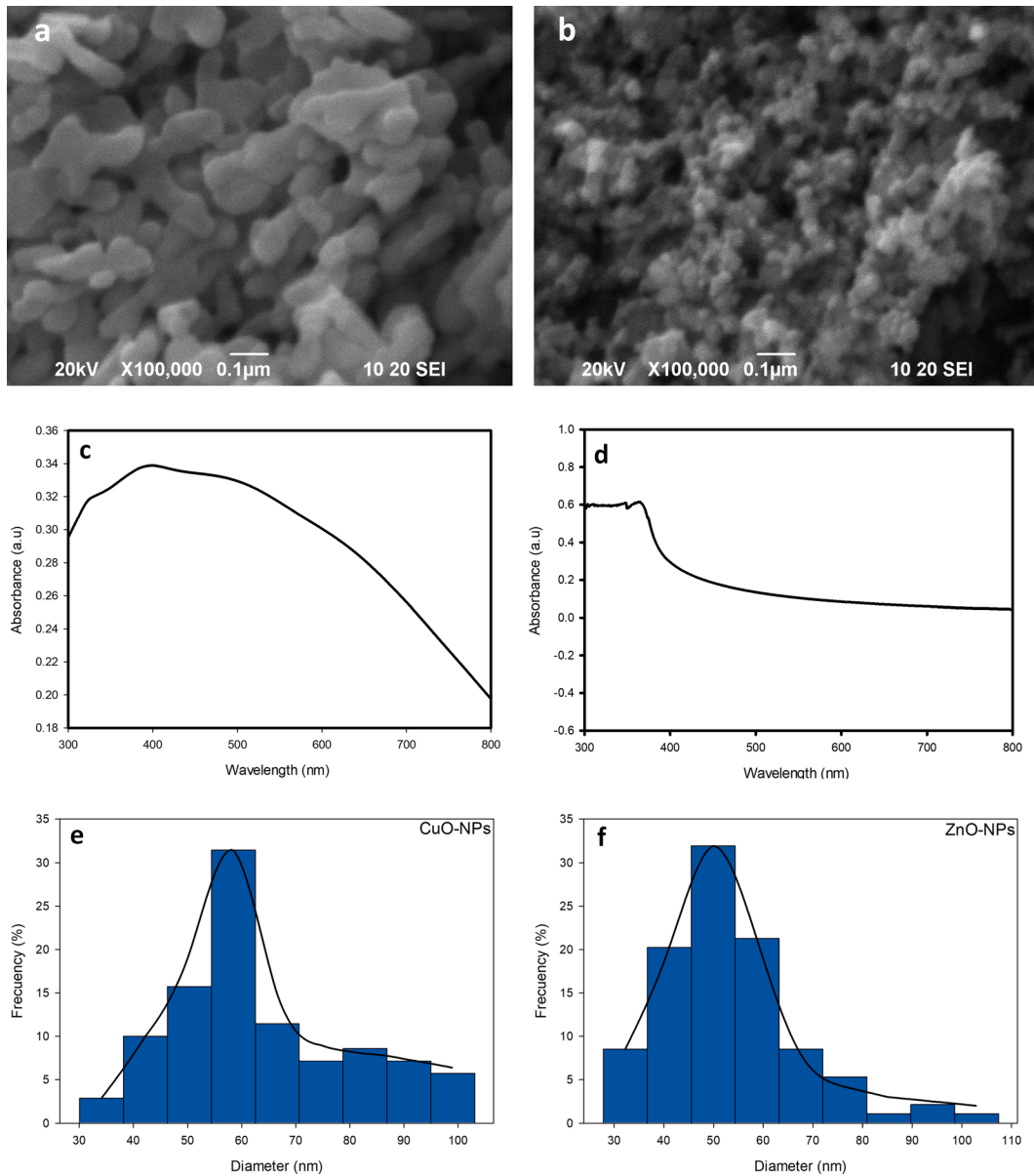


Fig. 2 SEM micrographs of CuO-NPs (a) and ZnO-NPs (b), with the respective UV–Vis spectrums, with absorption peak at 390 nm for CuO-NPs (c), and at 362 nm for ZnO-NPs (d). SEM diameter distribution histograms for CuO-NPs (e) and ZnO-NPs (f)

Table 1 Physicochemical properties of ZnO and CuO nanoparticles

Particles	Diameter (nm)		Hydrodynamic diameter (nm)	Polydispersity index (PDI)	Zeta potential (mV)
	Nominal	SEM			
CuO-NPs	50 nm	63.50 ± 16.78	220.43	0.320	-18.33
ZnO-NPs	50 nm	52.89 ± 14.46	223.00	0.366	8.15

3.3 Comet Assay

Figure 3 shows a summary of representative images of nuclei of *Taraxacum officinale* with different DNA damage obtained from comet assays for each treatment at two different times (rows), and all tested concentrations (columns) for each treatment, including negative and positive control. The higher intensities obtained by digital image analysis correspond to 100 mg/L for ZnO-NPs and 200 mg/L for CuO-NPs.

Three-way ANOVA of tail moments for ZnO and ZnO-NPs assays showed double interaction between factors, with statistically significant difference between treatments (ZnO, ZnO-NPs) and concentrations (negative control, 50, 100, 200, and 800 mg/L, positive control), treatments and time (24 h, and 5 days), and concentrations and time (Fig. 4). The significant difference between treatments confirms that the effects of plant exposure to Zn differs when the material comes in nanometric form (Fig. 4a). The effect of each concentration within both treatments showed a significant difference against the positive control, except for ZnO-NPs at 100 mg/L which presented no significant difference, corresponding with the concentration

that presented the maximum DNA damage, almost as toxic as this control. The comparison against negative control, suggest that the toxicity of ZnO-NPs is higher than that of ZnO, showing a significant difference for all concentrations, where ZnO only showed a difference against negative control at 800 mg/L. The analysis was similar for CuO and CuO-NPs (Fig. 4b), with no significant difference for all concentrations within CuO against negative control, and significant difference between treatments, confirming again the effects of the same material when presented in the nanometric form. In the same way, CuO-NPs suggest greater DNA damage when compared to bulk CuO treatment, with a significant differences against negative control for all concentrations from 100 mg/L. Comparison among concentrations within treatment and time is not possible since there was no triple interaction of factors. The effects of both ZnO-NPs and CuO-NPs treatments presented significant differences against their corresponding bulk counterparts at concentrations of 50, 100, and 200 mg/L, confirming the contribution of nanoparticles characteristics to DNA fragmentation. It is also likely that the aggregation of particles at higher concentrations when

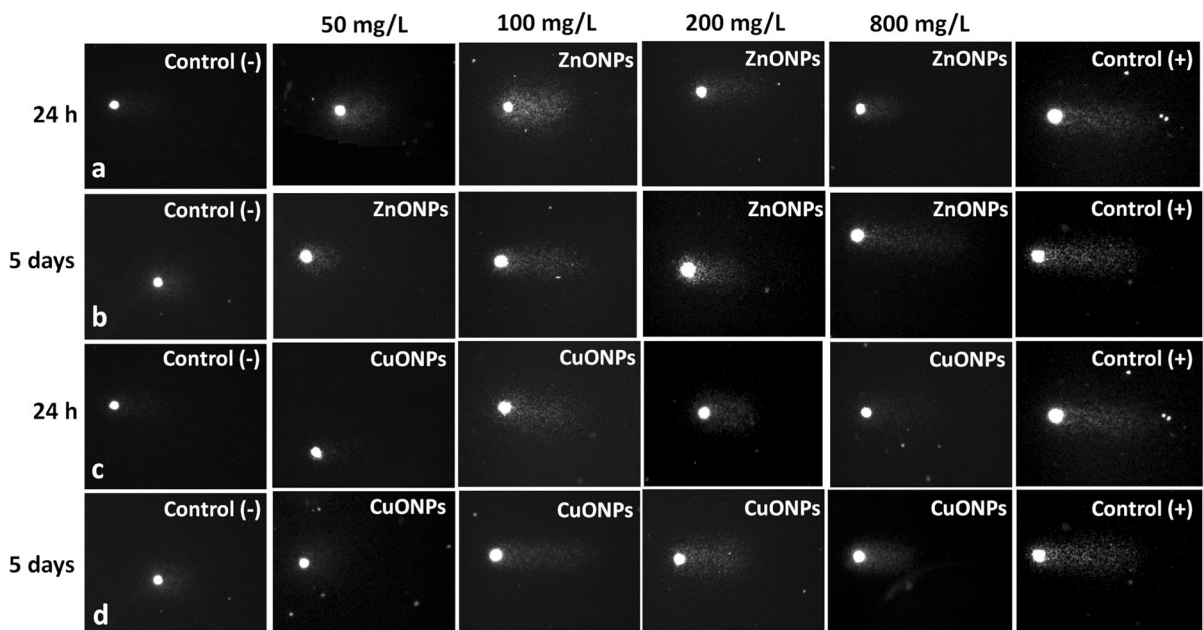
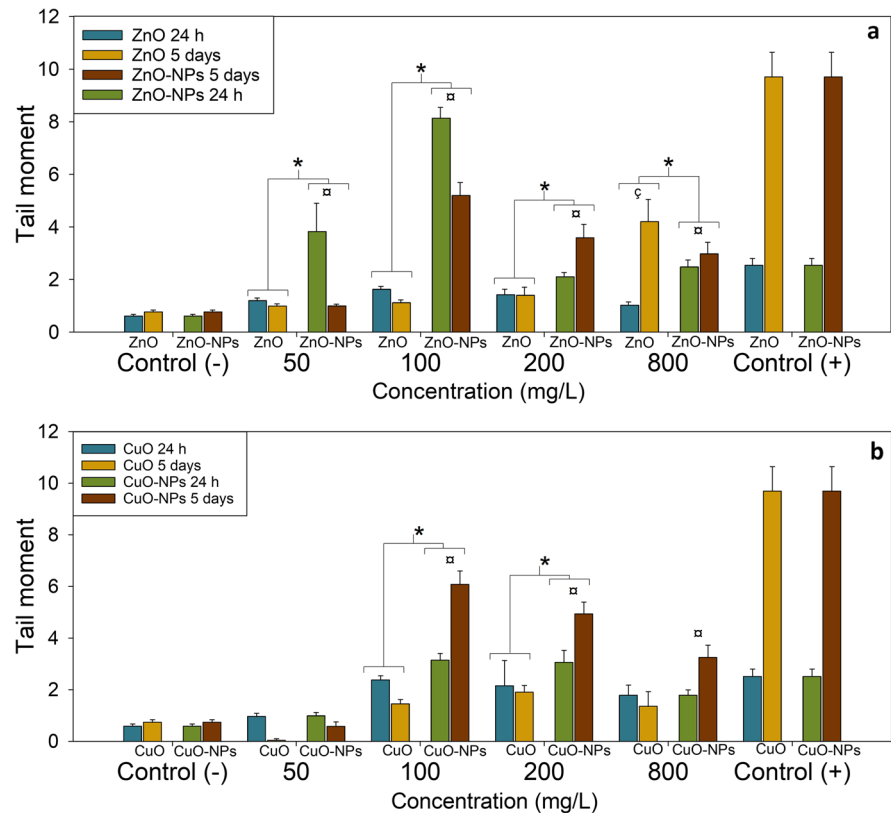


Fig. 3 Summary of representative comet assay images for each experiment set. Higher tail intensity is clearly visible for treatments at 100 mg/L for ZnO-NPs, 200 mg/L for CuO-NPs, and positive controls

Fig. 4 Genotoxicity results (tail moment) in *Taraxacum officinale* after exposure to ZnO-NPs (a), and CuO-NPs (b), compared against corresponding bulk material and controls. * Indicates significant difference between treatments within concentrations. ‡ Indicates significant difference against negative control within nanoparticle treatment. § Indicates significant difference against negative control within bulk treatment



interacting with the media reduces the effect of the nanometric form, as there were no significant differences at 800 mg/L.

Figure 5 summarizes the results of tail intensity (% tail DNA). Three-way ANOVA reported statistically significant interaction among the three factors: treatment, concentration, and time, for ZnO-NPs and ZnO, allowing the interpretation of interactions among concentrations, considering the variation of treatment and time; this comes as an important fact to consider the importance of reporting not only one parameter of the comet assay. There was no significant difference in tail intensity values among the different concentrations within bulk ZnO treatment at 24 h, in contrast to ZnO-NPs treatment (Fig. 5a), which reported significant differences for all concentrations with respect to the negative control, suggesting the genotoxic effects of the nanoparticles shortly after the exposure. 5 days after exposure (Fig. 5b), the effects on plants treated with ZnO presented a significant difference at 800 mg/L, ZnO-NPs treatment still showed a significant difference at 100 and 200 mg/L, but not at 50 and 800 mg/L. This suggests a reduction

in effects due to agglomeration of nanoparticles at the highest concentration, considering that their negative charge may be modified in the presence of organic matter (Keller et al., 2010), and presumably, that due to the lower effects at lower concentrations the DNA may be successfully repaired (Santos et al., 2015).

Despite ZnO is an essential micronutrient for plants, at excessive concentrations becomes toxic (Adhikari et al., 2020), as reported from the results at 5 days of exposure at 800 mg/L; ZnO-NPs at this same concentration may not present a significant toxicity due to the agglomeration and precipitation before uptake. CuO-NPs and CuO presented no triple interaction between factors, so significant differences are not labeled in the radar plot (Fig. 5c, d). None of the concentrations of CuO presented a significant difference against negative control, in contrast with CuO-NPs, where all concentrations but 50 mg/L presented significant differences, suggesting higher toxicity due to the properties of nanoparticles. In contrast to ZnO-NPs, the significant effect of CuO-NPs is still observed at a concentration of 800 mg/L after 5 days, suggesting better stability in accordance with

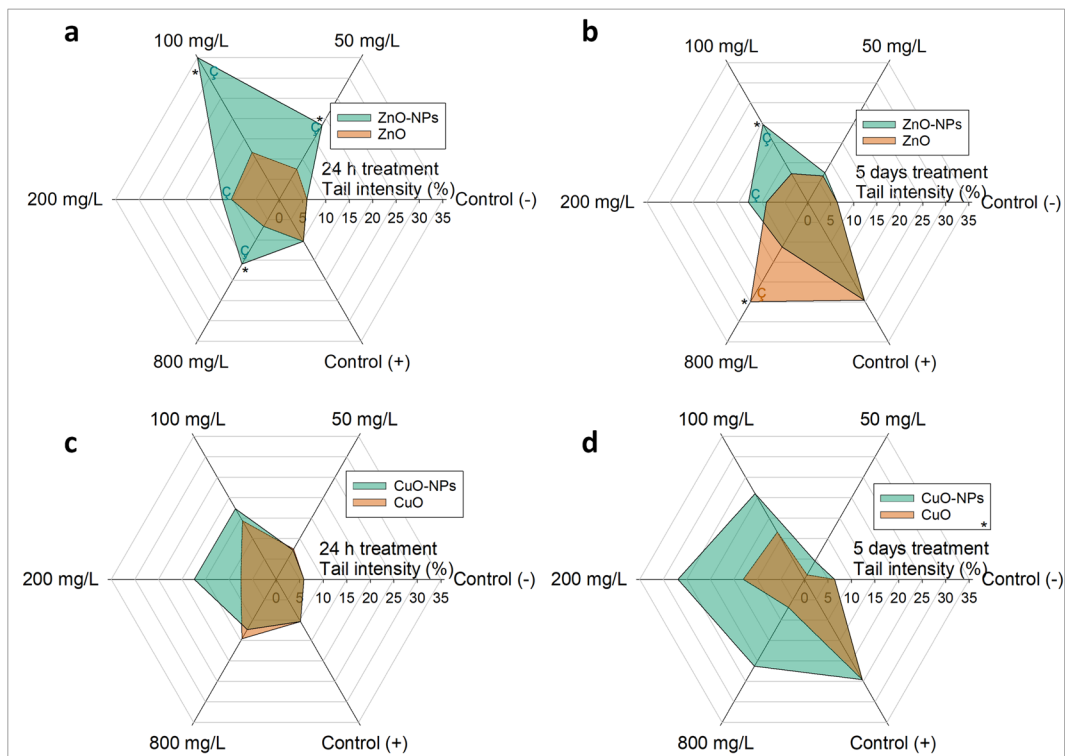


Fig. 5 Radar plot for tail intensity results of ZnO treatments after 24 h (a), and after 5 days (b), and CuO treatments after 24 h (c), and after 5 days (d). C Indicates significant difference

against negative control within treatment and time. * Indicates significant difference between treatments

zeta potential results. The statistically significant difference between the effects of bulk and nano cases for both CuO and ZnO at a concentration of 100 mg/L is always kept after considering the variation of the rest of the factors (time and concentration). Confirming again the importance of considering the potential damage caused by the pollution of nanostructured materials in comparison with the same materials in bulk form.

Figure 6 summarizes the results of tail length. There is statistically significant interaction among the three factors for ZnO and ZnO-NPs; data shows no significant difference for any concentration against negative control for neither ZnO or ZnO-NPs treatments at 24 h after exposure (Fig. 6a), but after 5 days (Fig. 6b), there is statistically significant difference for ZnO-NPs treatment at concentrations of 100, 200, and 800 mg/L. This may be explained by the fact that, in general, tail length presents high values when DNA breaks into pieces of single-stranded DNA of shorter lengths, corresponding to the long-term genotoxic

effects when higher number of breakages are present, this suggests the importance of studying the long-term effects of ZnO-NPs. Just as the data of tail intensity, ANOVA of CuO and CuO-NPs data presented no triple interaction between factors for tail length (Fig. 6c, d), none of the concentrations of CuO presented significant difference against negative control, and CuO-NPs, presented a significant difference for 100 and 200 mg/L, confirming higher toxicity against its bulk counterpart.

These results confirm the sensitivity of comet assay for the evaluation of genotoxicity of airborne ZnO and CuO nanoparticles with *Taraxacum officinale* as a bioindicator. The tail moment is a good parameter for the comparison of DNA damage between nano and bulk forms at different concentrations, and the tail intensity and tail length may be used to further describe genotoxic effects over time. All results confirm higher genotoxic effects of the nanoparticulate forms of CuO and ZnO treatment compared to their corresponding bulk counterpart,

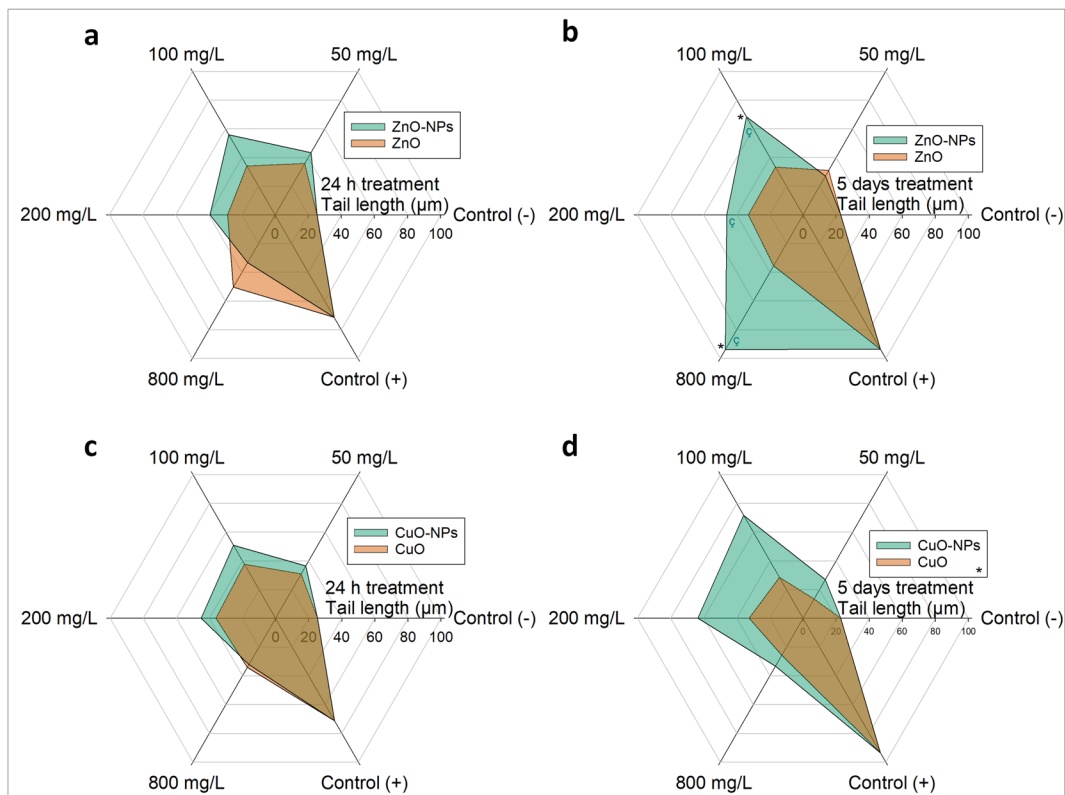


Fig. 6 Radar plots for tail length results of ZnO treatments after 24 h (a), and after 5 days (b), and CuO treatments after 24 h (c), and after 5 days (d). ζ Indicates significant difference

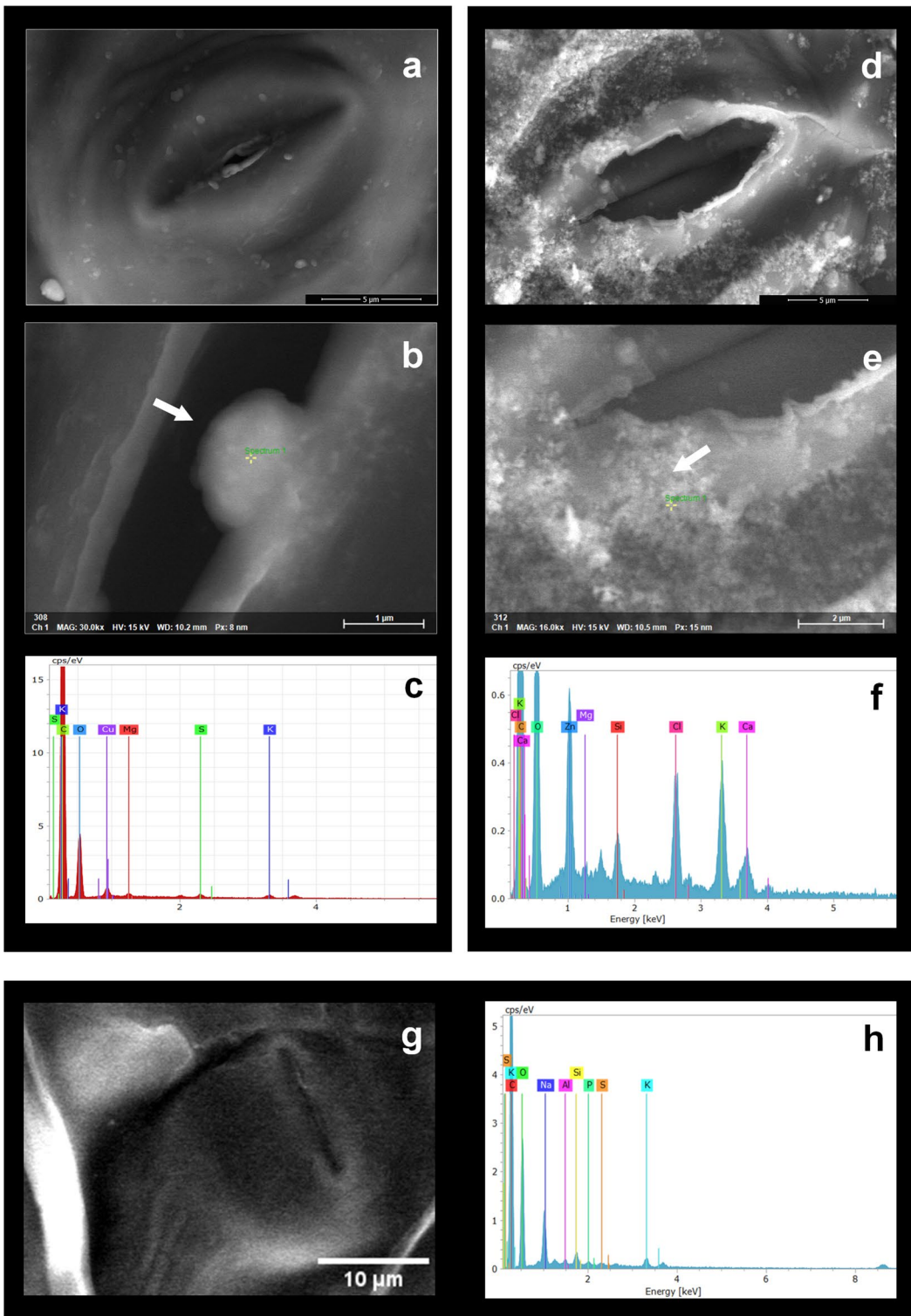
against negative control within treatment and time. * Indicates significant difference between treatments

except at the higher concentration, where the effect of nanoparticles treatments is not significantly different due to the low stability of nanoparticles dispersions at high concentrations, in accordance with previous results (Jo et al., 2012; Landsiedel et al., 2009). The statistically significant differences between stable dispersion of nanoparticles against bulk materials or unstable dispersions are confirmed too (Park et al., 2014).

Being the tail moment a more general parameter for the evaluation of genotoxicity, the three-way ANOVA results showed no triple interaction between treatments, concentration, and time; allowing only the description of significant differences among concentrations within treatments, excluding the effect of time; that is why, as reported in this work, it's recommended to include at least one of the other parameters obtained by the analysis of the comet assay images, i.e., tail intensity or tail length. As the statistical analysis of tail length and tail intensity results showed in

this work, *Taraxacum officinale* exhibited a higher genotoxic effect when exposed to ZnO and ZnO-NPs treatments; hence, significant interaction among the three tested factors was found, allowing the analysis of DNA damage considering the differences among concentrations for each treatment at specific times. This allows us to infer a successful DNA repair after the exposure at ZnO-NPs treatment at 50 and 800 mg/L after 5 days, since the differences of these concentrations against negative control are not significant, in contrast to the result obtained after 24 h where all concentrations were significantly different.

The higher DNA damage induced by ZnO-NPs at 100 mg/L and CuO-NPs at 200 mg/L reported by the tail intensity parameter of the comet assay could be explained by the uptake of nanoparticles through the leaves after the dissociation in the media as ions, forming complexes with organic compounds or causing oxidative stress (Adhikari et al., 2020). Other



causes of the toxicity after nanoparticles uptake may

◀**Fig. 7** SEM micrographs of stomata from leaves exposed to CuO-NPs (a), ZnO-NPs (d), and negative control (g). Points for EDS analysis for CuO-NPs (b) and ZnO-NP (e). EDS analysis displayed significant Cu (c) and Zn (f) peaks for leaves exposed to CuO-NPs and ZnO-NPs, respectively. Neither Cu nor Zn peaks are shown for the EDS of negative control samples (h)

be due to vacuole damage (Pokhrel & Dubey, 2013), and root length reduction (Ma et al., 2010a, b).

3.4 LV-SEM

Nanoparticles are observed at the surface of *Taraxacum officinale* leaves (Fig. 7) for both CuO-NPs (Fig. 7a) and ZnO-NPs (Fig. 7b) samples. ZnO-NPs showed higher agglomeration at the surface of leaves when compared to CuO-NPs, in accordance with the higher toxicity reported by comet assay. This may contribute to toxicity, as even when ZnO has been widely used in the formulation of fertilizers, it has been reported bioaccumulation in leaves and seeds (Siddiqi & Husen, 2017). Both CuO-NPs and ZnO-NPs are found more frequently near the stomata (a, b and c, d, respectively), which reduce their aperture when particles internalize; this has been reported before as an important cause of toxicity (Lv et al., 2019). Accumulation of agglomerates can be observed inside stomata (g, h), where the presence of Cu and Zn are confirmed by EDS analysis (i, j, and k, l, respectively); this may induce internalization. Following previous results, DNA damage may be induced by the internalization of nanoparticles through the stomata (Uzu et al., 2010; Večeřová et al., 2019; Zhao et al., 2017). Moreover, the impact of this internalization may be exacerbated under high atmospheric humidity conditions, which promote stomatal opening and increased nanoparticle intake. In situ studies have demonstrated this effect when comparing the results between rainy and dry seasons (Gómez-Arroyo et al., 2018b; Martínez-Pérez et al., 2021).

Zn mass percentage was 5.51%, measured at the point shown in Fig. 7i, and Cu mass percentage was 2.38%, measured at the point shown in Fig. 7k; the rest of the contents include mainly C and O, from the organic composition of samples, the low working vacuum, and the mounting tape. EDS spectra recorded at samples of leaves exposed to negative control showed mass percentage of Cu lower than 0.1%, and lower than 0.01% for Zn; this should be

considered part of the natural occurring micronutrients of plants (Cicek et al., 2022). For all cases, other elements (F, Ca, Cl, K, Mg) were found at very low percentages, high presence of Si is found too, up to 14%, due to the presence of soil dust and sand sediments. EDS of samples exposed to bulk materials, presented lower contents of Cu and Zn, around 0.37% and 1.36%, respectively.

3.5 Growth Rate

Figure 8 shows the mean growth rate of plants exposed to ZnO-NPs and Cu-NPs (bars), in comparison with positive and negative control (horizontal lines), and bulk form of ZnO, and CuO (straight lines and scatter). For concentrations of 100 mg/L and higher, both types of nanoparticles induced higher growth inhibition in comparison with their corresponding bulk form and the negative control. ZnO-NPs at 100 mg/L induced the highest growth inhibition, corresponding with the highest DNA damage obtained by comet assay. CuO-NPs seem to induce more growth inhibition as the concentration increases, in correspondence with tail intensity. Given that given that both Cu and Zn are common micronutrients of plants, we must consider that can be taken up after the release in ionic form, Cu is required in lower quantities than Zn, and it has been reported that the excessive release of Cu^{2+} ions affects the growth by causing oxidative damage (Da Costa et al., 2020). Sigmoidal dose–response curve fitting was used to calculate EC₅₀ for each treatment; ZnO-NPs and CuO-NPs presented lower EC₅₀ values, 50.86 and 65.84 mg/L respectively, in comparison with their bulk counterparts with higher values, being 100.30 mg/L for ZnO and 104.02 mg/L for CuO, making evident the higher toxic effects of nanoparticles than their corresponding bulk form. As reported by Adhikari et al. (2020) and Lee et al. (2010), ZnO-NPs dissolve faster than bulk ZnO, this, amid the presence of Zn^{2+} ions, may contribute with the higher toxicity of nanometric form of metal oxides, and the higher effects of ZnO-NPs when compared to other metal oxide NPs.

3.6 Total Chlorophyll Content

Figure 9 summarizes the quantification of chlorophyll 5 days after plant exposure. ZnO-NPs induced

Fig. 8 Growth rate at 5 days, relative to 24 h. Bars: ZnO-NPs and CuO-NPs. Scatter-lines: controls and bulk treatments

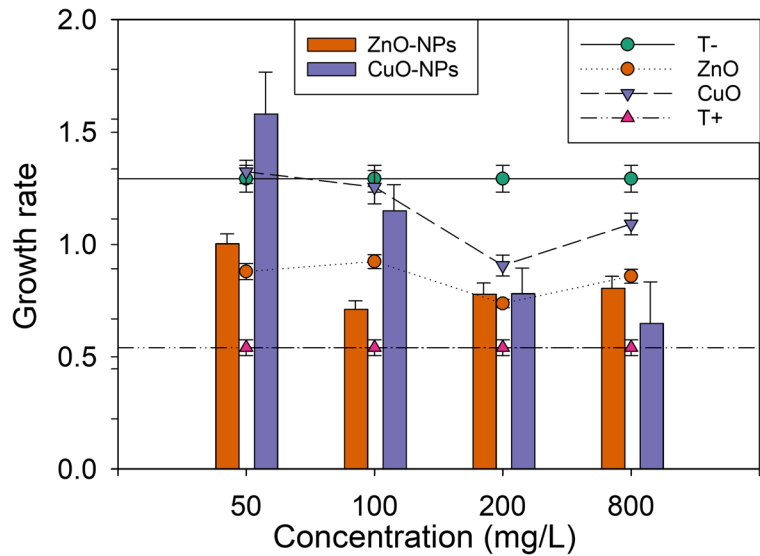
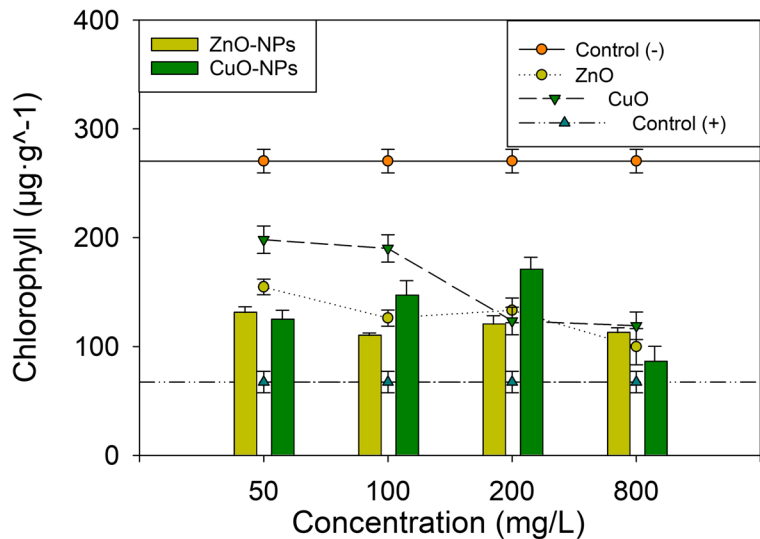


Fig. 9 Total chlorophyll. Bars: ZnO-NPs and CuO-NPs. Scatter-lines: controls and bulk treatments



the higher chlorosis at a concentration of 100 mg/L, in correspondence with the maximum DNA damage found by comet assay and growth inhibition; aside to the internalization of ZnO-NPs, their fast degradation could contribute to the substitution of the central atom of chlorophyll by Zn, inducing high chlorosis at this concentration (Mukherjee et al., 2014). CuO-NPs induced higher chlorosis at 800 mg/L, according to the higher growth inhibition. Two-way ANOVA reported a statistically significant interaction between the two factors (concentration and treatment) for both ZnO vs. ZnO-NPs, and CuO vs. CuO-NPs. All concentrations presented significant differences against

negative and positive controls within each treatment. For the case of ZnO-NPs, the chlorosis was very similar for all concentrations, with no statistically significant difference among all tested concentrations, excluding the controls.

The DNA damage caused by the studied NPs, probably reduces the expression of chlorophyll synthesis genes and structural genes of photosystem I, impacting the photosynthesis efficiency, next to the complexation of metal ions with phytochelatin that may break the balance between the metal uptake and fine tuning of cellular metal homeostasis pathways, just as reported by (Adhikari et al., 2020). In

the particular case of CuO-NPs, the quantification of chlorophyll showed higher chlorosis for the highest concentration; this effect may be caused not specifically by DNA damage but by the chemical degradation of chlorophyll in the presence of Cu, just as reported by Zhao et al. (2017). Given the valuable information obtained by chlorophyll content and growth inhibition, in addition to the genotoxic effects reported by comet assay, it is suggested to perform further studies with the inclusion of carotenoids level evaluation, as these pigments play important roles as scavengers of reactive oxygen species (Adhikari et al., 2020). The higher chlorophyll decline by exposure to CuO-NPs and ZnO-NPs may be explained too by a reduction of thylakoid stacking and distortion of the thylakoid membranes (Da Costa et al., 2020), effects that should be studied by advanced microscopy studies. Table 2 summarizes the obtained results of total chlorophyll and growth rate.

Aside from the DNA damage, the reported toxicity of both ZnO-NPs and CuO-NPs expressed by growth inhibition and chlorosis may be caused by the disturbing of important physiological processes of the plants due to the accumulation of nanoparticles near the stomata, as can be seen in LV-SEM results, followed by the penetration through this highly capacitive pathway or the clogging of the ostioles, as reported by (Uzu et al., 2010). Some studies about the distribution and dynamics of nanoparticles suggest the collapse of the vascular system after agglomeration (Cox et al., 2016); this may be the reason of the growth inhibition after exposure to highly concentrated dispersions of

nanoparticles. The reported results of growth inhibition and chlorosis are reinforced by the higher sensitivity of the comet assay to the nuclear DNA damage induced by exposure to nanoparticles, confirming the relevant role of this assay for the evaluation of emerging contaminants like nanomaterials, following recent studies (Santos et al., 2015).

4 Conclusions

This study validates the use of *Taraxacum officinale* as a bioindicator for the genotoxicity of nebulized dispersions of ZnO-NPs and CuO-NPs, as representative atmospheric nanostructured pollutants, taking advantage of the high sensitivity of the comet assay. The specific concentrations that cause greater DNA damage, as 100 mg/L for tail moment, may be taken as reference for further studies with other metal oxide nanoparticles, and the interaction of these concentrations with leaves surface should be further studied. SEM results demonstrate that nanoparticles dispersed in an atmosphere may accumulate in the surface of plant leaves, and, that the high humidity conditions may contribute to the agglomeration and internalization of nanoparticles through the stomata, increasing the genotoxicity, growth inhibition and chlorosis. The chlorosis results presented no significant difference among the tested concentrations for ZnO-NPs, but all of them indicate important damage to the photosynthesis efficiency as they present a significant difference against negative control, in contrast to the results

Table 2 Summary of total chlorophyll content and growth rate. * Indicates the higher chlorosis for each treatment. α indicates the higher growth inhibition for each treatment. ZnO-NPs induce higher chlorosis and growth inhibition at 100 mg/L

		Control (-)	50 mg/L	100 mg/L	200 mg/L	800 mg/L	Control (+)
Bulk ZnO	Total Chlorophyll ($\mu\text{g g}^{-1}$)	270.46	154.88	126.38	133.40	99.95*	67.39
	Growth rate	129.22	87.89	92.34	73.74 α	85.84	54.11
ZnO-NPs	Total Chlorophyll ($\mu\text{g g}^{-1}$)	270.46	131.50	110.40*	120.69	112.96	67.39
	Growth rate	129.22	90.01	63.77 α	69.88	72.21	54.11
Bulk CuO	Total Chlorophyll ($\mu\text{g g}^{-1}$)	270.46	198.21	190.21	123.66	119.29*	67.39
	Growth rate	129.22	132.35	125.50	90.59 α	109.06	54.11
CuO-NPs	Total Chlorophyll ($\mu\text{g g}^{-1}$)	270.46	125.13	147.36	170.96	86.35*	67.39
	Growth rate	129.22	142.00	103.23	70.09	58.14 α	54.11

obtained by comet assay, that proved to be more sensitive to the tested concentrations. In the case of CuO-NPs, the level of chlorosis at 800 mg/L presents the highest difference against the rest of the concentrations, this may be due to the direct degradation of chlorophyll by the interaction with CuO. The concentration-dependent growth inhibition and chlorosis is clear, this has important ecotoxicological implications that should be investigated given the capacity of this kind of nanoparticles to induce oxidative stress and DNA damage.

Comet assay, in contrast, presented significant differences among most of the tested concentrations, suggesting a high sensitivity of the method to evaluate the toxicity of nanoparticles using plants as bioindicators. According to the obtained results, it is recommended to consider the three parameters of the comet assay, tail moment, tail intensity, and tail length, as each one provides valuable information depending on the sensitivity of the bioindicator and the characteristics of the evaluated material. Tail length proved to be most significant to investigate the long-term effects of nanoparticles on plants, as it gives high values 5 days after plant exposure. The DNA damage induced by the lower tested concentrations of CuO-NPs and ZnO-NPs has an effect that persists over time, as confirmed by the results obtained from the assays performed after 5 days. This suggests the need to perform further studies of the genotoxic effects of metal oxide nanoparticles, extending the studies of comet assay with other bioindicators, considering the possible changes in the tolerance to different kind of particles across species.

Acknowledgements The authors thank the support the Instituto de Ciencias de la Atmósfera y Cambio Climático, Universidad Nacional Autónoma de México (UNAM), and the Instituto Politécnico Nacional (IPN), both for the resources and facilities granted to carry out this research. To the Dirección de Asuntos del Personal Académico (DGPA), UNAM, for the postdoctoral fellowship awarded to Paulina Abrica González. To Centro de Nanociencias y Micro y Nanotecnologías, IPN, for SEM analysis, and the Red Universitaria de Observatorios Atmosféricos, UNAM, for the atmospheric sensors and data.

Author Contribution All authors contributed to the study conception and design. Material preparation, data collection, and data analysis were performed by Abrica-González, P., Flores-Márquez, A., Sotelo-López, A., and Cortés-Eslava, J. Research management and final revision on data and manuscript were performed by Gómez-Arroyo, S. and Jazcilevich-Diamant, A. All authors commented on previous versions

of the manuscript. All authors read and approved the final manuscript.

Data Availability The datasets are available from the corresponding author on request.

Declarations

Competing Interests The authors declare no competing interests.

Open Access This article is licensed under a Creative Commons Attribution 4.0 International License, which permits use, sharing, adaptation, distribution and reproduction in any medium or format, as long as you give appropriate credit to the original author(s) and the source, provide a link to the Creative Commons licence, and indicate if changes were made. The images or other third party material in this article are included in the article's Creative Commons licence, unless indicated otherwise in a credit line to the material. If material is not included in the article's Creative Commons licence and your intended use is not permitted by statutory regulation or exceeds the permitted use, you will need to obtain permission directly from the copyright holder. To view a copy of this licence, visit <http://creativecommons.org/licenses/by/4.0/>.

References

- Abrica-González, P., Zamora-Justo, J. A., Chávez-Sandoval, B. E., Vázquez-Martínez, G. R., & Balderas-López, J. A. (2018). Measurement of the optical properties of gold colloids by photoacoustic spectroscopy. *International Journal of Thermophysics*, 39(8), 93. <https://doi.org/10.1007/s10765-018-2412-1>
- Adamczyk-Szabela, D., Lisowska, K., & Wolf, W. M. (2021). Hysteresis of heavy metals uptake induced in *Taraxacum officinale* by thiuram. *Scientific Reports*, 11(1), 20151. <https://doi.org/10.1038/s41598-021-99666-2>
- Adhikari, S., Adhikari, A., Ghosh, S., Roy, D., Azahar, I., Basuli, D., & Hossain, Z. (2020). Assessment of ZnO-NPs toxicity in maize: An integrative microRNAomic approach. *Chemosphere*, 249, 126197. <https://doi.org/10.1016/j.chemosphere.2020.126197>
- Bozdogan Sert, E., Turkmen, M., & Cetin, M. (2019). Heavy metal accumulation in rosemary leaves and stems exposed to traffic-related pollution near Adana-İskenderun Highway (Hatay, Turkey). *Environmental Monitoring and Assessment*, 191(9), 553. <https://doi.org/10.1007/s10661-019-7714-7>
- Bystrzejewska-Piotrowska, G., Golimowski, J., & Urban, P. L. (2009). Nanoparticles: Their potential toxicity, waste and environmental management. *Waste Management*, 29(9), 2587–2595. <https://doi.org/10.1016/j.wasman.2009.04.001>
- Cetin, M. (2013). Landscape engineering, protecting soil, and runoff storm water. In M. Özyavuz (Ed.), *Advances in*

- landscape architecture. InTechOpen. <https://doi.org/10.5772/55812>
- Cetin, M. (2015a). Using GIS analysis to assess urban green space in terms of accessibility: Case study in Kutahya. *International Journal of Sustainable Development & World Ecology*, 22(5), 1–5. <https://doi.org/10.1080/13504509.2015.1061066>
- Cetin, M. (2015b). Evaluation of the sustainable tourism potential of a protected area for landscape planning: A case study of the ancient city of Pompeopolis in Kastamonu. *International Journal of Sustainable Development & World Ecology*, 22(6), 490–495. <https://doi.org/10.1080/13504509.2015.1081651>
- Cetin, M. (2016a). A change in the amount of CO₂ at the center of the examination halls: Case study of Turkey. *Studies on Ethno-Medicine*, 10(2), 146–155. <https://doi.org/10.1080/09735070.2016.11905483>
- Cetin, M. (2016b). Sustainability of urban coastal area management: A case study on Cide. *Journal of Sustainable Forestry*, 35(7), 527–541. <https://doi.org/10.1080/10549811.2016.1228072>
- Cetin, M., & Asghar Jawed, A. (2021). The chancing of Mg concentrations in some plants grown in Pakistan depends on plant species and the growing environment. *Kastamonu University Journal of Engineering and Sciences*, 7(2), 167–174.
- Cetin, M., Isik Pekkan, O., Bilge Ozturk, G., Senyel Kurkcuoğlu, M. A., Kucukpehlivan, T., & Cabuk, A. (2022a). Examination of the change in the vegetation around the Kirka boron mine site by using remote sensing techniques. *Water, Air, & Soil Pollution*, 233(7), 254. <https://doi.org/10.1007/s11270-022-05738-y>
- Cetin, M., Aljama, A. M. O., Alrabiti, O. B. M., Adiguzel, F., Sevik, H., & Zeren Cetin, I. (2022b). Determination and mapping of regional change of Pb and Cr pollution in Ankara City Center. *Water, Air, & Soil Pollution*, 233(5), 163. <https://doi.org/10.1007/s11270-022-05638-1>
- Cetin, M., Aljama, A. M. O., Alrabiti, O. B. M., Adiguzel, F., Sevik, H., & Zeren Cetin, I. (2022c). Using topsoil analysis to determine and map changes in Ni Co pollution. *Water, Air, & Soil Pollution*, 233(8), 293. <https://doi.org/10.1007/s11270-022-05762-y>
- Cetin, M., & Asghar Jawed, A. (2022). Variation of Ba concentrations in some plants grown in Pakistan depending on traffic density. *Biomass Conversion and Biorefinery*, 0123456789. <https://doi.org/10.1007/s13399-022-02334-2>
- Cicek, N., Erdogan, M., Yucedag, C., & Cetin, M. (2022). Improving the detrimental aspects of salinity in salinized soils of arid and semi-arid areas for effects of vermicompost leachate on salt stress in seedlings. *Water, Air, & Soil Pollution*, 233(6), 197. <https://doi.org/10.1007/s11270-022-05677-8>
- Coelho, M. C., Torráo, G., Emami, N., & Grácio, J. (2012). Nanotechnology in automotive industry: Research strategy and trends for the future-small objects, big impacts. *Journal of Nanoscience and Nanotechnology*, 12(8), 6621–6630. <https://doi.org/10.1166/jnn.2012.4573>
- Cortés-Eslava, J., Gómez-Arroyo, S., Risueño, M. C., & Testillano, P. S. (2018). The effects of organophosphorus insecticides and heavy metals on DNA damage and programmed cell death in two plant models. *Environmental Pollution*, 240, 77–86. <https://doi.org/10.1016/j.envpol.2018.04.119>
- Cortés-Eslava, J., Gómez-Arroyo, S., Mérida Cortés, P. A., Jiménez-García, L. F., Lara-Martínez, R., Arenas-Huertero, F., Morton-Bermea, O., & Testillano, P. S. (2023). The wild plant *Gnaphalium lavandulifolium* as a sentinel for biomonitoring the effects of environmental heavy metals in the metropolitan area of México Valley. *Environmental and Monitoring Assessment*, 195, 195. <https://doi.org/10.1007/s10661-022-10763-9>
- Cox, A., Venkatachalam, P., Sahi, S., & Sharma, N. (2016). Silver and titanium dioxide nanoparticle toxicity in plants: A review of current research. *Plant Physiology and Biochemistry*, 107, 147–163. <https://doi.org/10.1016/j.plaphy.2016.05.022>
- Da Costa, M. V. J., Kevat, N., & Sharma, P. K. (2020). Copper oxide nanoparticle and copper (II) ion exposure in *Oryza sativa* reveals two different mechanisms of toxicity. *Water, Air, & Soil Pollution*, 231(6), 258. <https://doi.org/10.1007/s11270-020-04592-0>
- Dailey, L. A., Schmehl, T., Gessler, T., Wittmar, M., Griminger, F., Seeger, W., & Kissel, T. (2003). Nebulization of biodegradable nanoparticles: Impact of nebulizer technology and nanoparticle characteristics on aerosol features. *Journal of Controlled Release*, 86(1), 131–144. [https://doi.org/10.1016/S0168-3659\(02\)00370-X](https://doi.org/10.1016/S0168-3659(02)00370-X)
- Degórska, A. (2013). An assessment of urban habitat contamination with selected heavy metals within the city of Katowice using the common dandelion (*Taraxacum officinale* Web.) as a bioindicator. *Environmental & Socio-Economic Studies*, 1(4), 29–40. <https://doi.org/10.1515/envir-on-2015-0021>
- Dong, B., Ikonnikova, I., Rogulin, R., Sakulyeva, T., & Mikhaylov, A. (2021). Environmental-economic approach to optimization of transport communication in megacities. *Journal of Environmental Science and Health, Part A*, 56(6), 660–666. <https://doi.org/10.1080/10934529.2021.1913928>
- Dzierzanowski, K., Popek, R., Gawrońska, H., Sæbø, A., & Gawroński, S. W. (2011). Deposition of particulate matter of different size fractions on leaf surfaces and in waxes of urban forest species. *International Journal of Phytoremediation*, 13(10), 1037–1046. <https://doi.org/10.1080/15226514.2011.552929>
- Gichner, T., & Plewa, M. J. (1998). Induction of somatic DNA damage as measured by single cell gel electrophoresis and point mutation in leaves of tobacco plants. *Mutation Research/fundamental and Molecular Mechanisms of Mutagenesis*, 401(1–2), 143–152. [https://doi.org/10.1016/S0027-5107\(98\)00003-7](https://doi.org/10.1016/S0027-5107(98)00003-7)
- Gómez-Arroyo, S., Barba-García, A., Arenas-Huertero, F., Cortés-Eslava, J., de la Mora, M. G., & García-Martínez, R. (2018a). Indicators of environmental contamination by heavy metals in leaves of *Taraxacum officinale* in two zones of the metropolitan area of Mexico City. *Environmental Science and Pollution Research*, 25(5), 4739–4749. <https://doi.org/10.1007/s11356-017-0809-1>
- Gómez-Arroyo, S., Cortés-Eslava, J., Loza-Gómez, P., Arenas-Huertero, F., Grutter de la Mora, M., & Morton Bermea, O. (2018b). In situ biomonitoring of air quality in rural and urban environments of Mexico Valley through

- genotoxicity evaluated in wild plants. *Atmospheric Pollution Research*, 9(1), 119–125. <https://doi.org/10.1016/j.apr.2017.06.009>
- Ibrahim, R. K., Hayyan, M., AlSaadi, M. A., Hayyan, A., & Ibrahim, S. (2016). Environmental application of nanotechnology: Air, soil, and water. *Environmental Science and Pollution Research*, 23(14), 13754–13788. <https://doi.org/10.1007/s11356-016-6457-z>
- Jo, H. J., Choi, J. W., Lee, S. H., & Hong, S. W. (2012). Acute toxicity of Ag and CuO nanoparticle suspensions against *Daphnia magna*: The importance of their dissolved fraction varying with preparation methods. *Journal of Hazardous Materials*, 227–228, 301–308. <https://doi.org/10.1016/j.jhazmat.2012.05.066>
- Karlsson, H. L. (2010). The comet assay in nanotoxicology research. *Analytical and Bioanalytical Chemistry*, 398(2), 651–666. <https://doi.org/10.1007/s00216-010-3977-0>
- Keller, A. A., Wang, H., Zhou, D., Lenihan, H. S., Cherr, G., Cardinale, B. J., Miller, R., & Ji, Z. (2010). Stability and aggregation of metal oxide nanoparticles in natural aqueous matrices. *Environmental Science & Technology*, 44(6), 1962–1967. <https://doi.org/10.1021/es902987d>
- Khan, A., Ali, H. M., Nazir, R., Ali, R., Munir, A., Ahmad, B., & Ahmad, Z. (2019). Experimental investigation of enhanced heat transfer of a car radiator using ZnO nanoparticles in H₂O–ethylene glycol mixture. *Journal of Thermal Analysis and Calorimetry*, 138(5), 3007–3021. <https://doi.org/10.1007/s10973-019-08320-7>
- Khataee, A., Movafeghi, A., Mojaver, N., Vafaei, F., Tarrahi, R., & Dadpour, M. R. (2017). Toxicity of copper oxide nanoparticles on *Spirodela polyrrhiza*: Assessing physiological parameters. *Research on Chemical Intermediates*, 43(2), 927–941. <https://doi.org/10.1007/s11164-016-2674-9>
- Kumar, R., Youssry, S. M., Abdel-Galeil, M. M., & Matsuda, A. (2020). One-pot synthesis of reduced graphene oxide nanosheets anchored ZnO nanoparticles via microwave approach for electrochemical performance as supercapacitor electrode. *Journal of Materials Science: Materials in Electronics*, 31(18), 15456–15465. <https://doi.org/10.1007/s10854-020-04108-w>
- Landsiedel, R., Kapp, M. D., Schulz, M., Wiench, K., & Oesch, F. (2009). Genotoxicity investigations on nanomaterials: Methods, preparation and characterization of test material, potential artifacts and limitations—many questions, some answers. *Mutation Research/reviews in Mutation Research*, 681(2–3), 241–258. <https://doi.org/10.1016/j.mrrev.2008.10.002>
- Lee, C. W., Mahendra, S., Zodrow, K., Li, D., Tsai, Y.-C., Braam, J., & Alvarez, P. J. J. (2010). Developmental phytotoxicity of metal oxide nanoparticles to *Arabidopsis thaliana*. *Environmental Toxicology and Chemistry*, 29(3), 669–675. <https://doi.org/10.1002/etc.58>
- Lin, D., Tian, X., Wu, F., & Xing, B. (2010). Fate and transport of engineered nanomaterials in the environment. *Journal of Environmental Quality*, 39(6), 1896–1908. <https://doi.org/10.2134/jeq2009.0423>
- Lv, J., Christie, P., & Zhang, S. (2019). Uptake, translocation, and transformation of metal-based nanoparticles in plants: Recent advances and methodological challenges. *Environmental Science: Nano*, 6(1), 41–59. <https://doi.org/10.1039/C8EN00645H>
- Ma, X., Geiser-Lee, J., Deng, Y., & Kolmakov, A. (2010a). Interactions between engineered nanoparticles (ENPs) and plants: Phytotoxicity, uptake and accumulation. *Science of the Total Environment*, 408(16), 3053–3061. <https://doi.org/10.1016/j.scitotenv.2010.03.031>
- Ma, Y., Kuang, L., He, X., Bai, W., Ding, Y., Zhang, Z., Zhao, Y., & Chai, Z. (2010b). Effects of rare earth oxide nanoparticles on root elongation of plants. *Chemosphere*, 78(3), 273–279. <https://doi.org/10.1016/j.chemosphere.2009.10.050>
- Martínez, G., Merinero, M., Pérez-Aranda, M., Pérez-Soriano, E., Ortiz, T., Villamor, E., Begines, B., & Alcudia, A. (2020). Environmental impact of nanoparticles' application as an emerging technology: A review. *Materials*, 14(7), 1710. <https://doi.org/10.3390/ma14010166>
- Martínez-Pérez, M., Arenas-Huertero, F., Cortés-Eslava, J., Morton-Bermea, O., & Gómez-Arroyo, S. (2021). *Robinsonia gerberifolia* as a sentinel organism for atmospheric pollution by heavy metals in several zones of Mexico City and its metropolitan area. *Environmental Science and Pollution Research*, 28, 31032–31042. <https://doi.org/10.1007/s11356-021-12862-5>
- Miri, A., Mahdinejad, N., Ebrahimi, O., Khatami, M., & Sarani, M. (2019). Zinc oxide nanoparticles: Biosynthesis, characterization, antifungal and cytotoxic activity. *Materials Science and Engineering: C*, 104, 109981. <https://doi.org/10.1016/j.msec.2019.109981>
- Morales, V. L., Sang, W., Fuka, D. R., Lion, L. W., Gao, B., & Steenhuis, T. S. (2011). Correlation equation for predicting attachment efficiency (α) of organic matter-colloid complexes in unsaturated porous media. *Environmental Science & Technology*, 45(23), 10096–10101. <https://doi.org/10.1021/es2023829>
- Mukherjee, A., Peralta-Video, J. R., Bandyopadhyay, S., Rico, C. M., Zhao, L., & Gardea-Torresdey, J. L. (2014). Physiological effects of nanoparticulate ZnO in green peas (*Pisum sativum* L.) cultivated in soil. *Metallomics*, 6(1), 132–138. <https://doi.org/10.1039/C3MT00064H>
- Nabila, M. I., & Kannabiran, K. (2018). Biosynthesis, characterization and antibacterial activity of copper oxide nanoparticles (CuO NPs) from actinomycetes. *Biocatalysis and Agricultural Biotechnology*, 15, 56–62. <https://doi.org/10.1016/j.bcab.2018.05.011>
- Navada, K. M., Nagaraja, G. K., D'Souza, J. N., Kouser, S., Ranjitha, R., & Manasa, D. J. (2020). Phyto assisted synthesis and characterization of *Scoparia dulcis* L. leaf extract mediated porous nano CuO photocatalysts and its anticancer behavior. *Applied Nanoscience*, 10(11), 4221–4240. <https://doi.org/10.1007/s13204-020-01536-2>
- Park, S., Woodhall, J., Ma, G., Veinot, J. G. C., Cresser, M. S., & Boxall, A. B. A. (2014). Regulatory ecotoxicity testing of engineered nanoparticles: Are the results relevant to the natural environment? *Nanotoxicology*, 8(5), 583–592. <https://doi.org/10.3109/17435390.2013.818173>
- Parmar, T. K., Rawtani, D., & Agrawal, Y. K. (2016). Bioindicators: The natural indicator of environmental pollution. *Frontiers in Life Science*, 9(2), 110–118. <https://doi.org/10.1080/21553769.2016.1162753>

- Pokhrel, L. R., & Dubey, B. (2013). Evaluation of developmental responses of two crop plants exposed to silver and zinc oxide nanoparticles. *Science of the Total Environment*, 452–453, 321–332. <https://doi.org/10.1016/j.scitotenv.2013.02.059>
- Rahman, A., & Myo Aung, K. (2021). Development of solar supercapacitor by utilizing organic polymer and metal oxides for subsystem of EV. *Materials Research Express*, 8(12), 125301. <https://doi.org/10.1088/2053-1591/ac3ce9>
- Rotini, A., Tornambè, A., Cossi, R., Iamunno, F., Benvenuto, G., Berducci, M. T., Maggi, C., Thaller, M. C., Cicero, A. M., Manfra, L., & Migliore, L. (2017). Salinity-based toxicity of CuO nanoparticles, CuO-bulk and Cu ion to *Vibrio anguillarum*. *Frontiers in Microbiology*, 8. <https://doi.org/10.3389/fmicb.2017.02076>
- Santos, C. L. V., Pourrut, B., & Ferreira de Oliveira, J. M. P. (2015). The use of comet assay in plant toxicology: Recent advances. *Frontiers in Genetics*, 6. <https://doi.org/10.3389/fgene.2015.00216>
- Shafique, M., & Luo, X. (2019). Nanotechnology in transportation vehicles: An overview of its applications, environmental, health and safety concerns. *Materials*, 12(15), 2493. <https://doi.org/10.3390/ma12152493>
- Shah, R., Gashi, B., & Rosenkranz, A. (2022). Latest developments in designing advanced lubricants and greases for electric vehicle-An overview. *Lubrication Science*, 34(8), 515–526. <https://doi.org/10.1002/ls.1605>
- Sharaf Zeebaree, S. Y., Sharaf Zeebaree, A. Y., Haji Zebari, O. I., & Sharaf Zebari, A. Y. (2021). Sustainable fabrication, optical properties and rapid performance of bio-engineered copper nanoparticles in removal of toxic methylene blue dye in an aqueous medium. *Current Research in Green and Sustainable Chemistry*, 4, 100103. <https://doi.org/10.1016/j.crgsc.2021.100103>
- Siddiqi, K. S., & Husen, A. (2017). Plant response to engineered metal oxide nanoparticles. *Nanoscale Research Letters*, 12(1), 92. <https://doi.org/10.1186/s11671-017-1861-y>
- Tripathi, D. K., Shweta, Singh, S., Singh, S., Pandey, R., Singh, V. P., Sharma, N. C., Prasad, S. M., Dubey, N. K., & Chauhan, D. K. (2017). An overview on manufactured nanoparticles in plants: Uptake, translocation, accumulation and phytotoxicity. *Plant Physiology and Biochemistry*, 110, 2–12. <https://doi.org/10.1016/j.plaphy.2016.07.030>
- Uzu, G., Sobanska, S., Sarret, G., Muñoz, M., & Dumat, C. (2010). Foliar lead uptake by lettuce exposed to atmospheric fallouts. *Environmental Science & Technology*, 44(3), 1036–1042. <https://doi.org/10.1021/es902190u>
- Van Dyck, L., Bentouhami, H., Koch, K., Samson, R., & Weyler, J. (2019). Exposure to indoor ferromagnetic particulate matter monitored by strawberry plants and the occurrence of acute respiratory events in adults. *International Journal of Environmental Research and Public Health*, 16(23), 4823. <https://doi.org/10.3390/ijerph16234823>
- Večeřová, K., Večeřa, Z., Mikuška, P., Coufalík, P., Oravec, M., Dočekal, B., Novotná, K., Veselá, B., Pompeiano, A., & Urban, O. (2019). Temperature alters susceptibility of *Picea abies* seedlings to airborne pollutants: The case of CdO nanoparticles. *Environmental Pollution*, 253, 646–654. <https://doi.org/10.1016/j.envpol.2019.07.061>
- Wang, P., Menzies, N. W., Lombi, E., McKenna, B. A., Johannessen, B., Glover, C. J., Kappen, P., & Kopittke, P. M. (2013). Fate of ZnO nanoparticles in soils and cowpea (*Vigna unguiculata*). *Environmental Science & Technology*, 47(23), 13822–13830. <https://doi.org/10.1021/es403466p>
- Wang, Z., Xu, L., Zhao, J., Wang, X., White, J. C., & Xing, B. (2016). CuO nanoparticle interaction with *Arabidopsis thaliana*: Toxicity, parent-progeny transfer, and gene expression. *Environmental Science & Technology*, 50(11), 6008–6016. <https://doi.org/10.1021/acs.est.6b01017>
- Wei, H., & Wang, E. (2013). Nanomaterials with enzyme-like characteristics (nanozymes): Next-generation artificial enzymes. *Chemical Society Reviews*, 42(14), 6060. <https://doi.org/10.1039/c3cs35486e>
- Yuvarajan, D., Dinesh Babu, M., BeemKumar, N., & Amith Kishore, P. (2018). Experimental investigation on the influence of titanium dioxide nanofluid on emission pattern of biodiesel in a diesel engine. *Atmospheric Pollution Research*, 9(1), 47–52. <https://doi.org/10.1016/j.apr.2017.06.003>
- Zhao, J., Ren, W., Dai, Y., Liu, L., Wang, Z., Yu, X., Zhang, J., Wang, X., & Xing, B. (2017). Uptake, distribution, and transformation of CuO NPs in a floating plant *Eichhornia crassipes* and related stomatal responses. *Environmental Science & Technology*, 51(13), 7686–7695. <https://doi.org/10.1021/acs.est.7b01602>

Publisher's Note Springer Nature remains neutral with regard to jurisdictional claims in published maps and institutional affiliations.